Velocity Constrained Time-Optimal Control of a Gantry Crane System

Adrian Stein¹ and Tarunraj Singh²

Abstract—The focus of this paper is on the development of velocity constrained time-optimal control profiles for point-to-point motion of a gantry crane system. Assuming that the velocity of the trolley of the crane can be commanded, an optimal control problem is posed to determine the bang-off-bang control profile to transition the system to the terminal states with no residual vibrations. Both undamped and underdamped systems are considered and the variation of the structure of the optimal control profiles as a function of the final displacement is studied and the collapse and birthing of switches in the control profile are explained. To account for uncertainties in model parameters, a robust controller design is posed and the tradeoff of increase in maneuver time to the reduction of residual vibrations is illustrated.

 ${\it Index~Terms} {\color{red} --} \ {\bf Input~Shaper,~Gantry~Crane,~Vibration~Control.}$

I. INTRODUCTION

Control of cranes has been a topic garnering increasing interest over the past three decades with the growth in the use of prefiltering approaches to minimize residual vibrations of systems characterized by underdamped motion. One such approach is called input shaping which consists of a timedelay filter which is designed to cancel the underdamped poles of the system. To account for uncertainties in the estimated damping or natural frequencies of the underdamped poles, multiple zeros of the time-delay filter are located at the nominal location of the underdamped poles, resulting in robustness to uncertainties in the modal parameters. The domain of input shaping has matured and can account for uncertainties by desensitizing the time-delay filter around the nominal model [1] or by accounting for the interval domains of uncertainties [2]. Constraints on jerk [3], deflection [4] have also been taken into account in the design. Including time-delay filters inside the feedback loop [5] and distributed delay input shapers [6] have also been studied which are novel deployment of input shapers.

Noakes, Petterson, and Werner [7] proposed a switching control profile to generate oscillation-damped transport and swing-free stop. Their technique consists of bang-off-bang acceleration profiles in which the pulses are timed to minimize the cable sway during the maneuver and results in a swing-free stop. They experimentally demonstrated the results of the open-loop control design. Fliess, Levine, and Rouchon [8] used the concept of differential flatness to control the traversing and hoisting of an overhead crane. They proposed tracking a C4 smooth reference profile to minimize the oscillations of the cable during the maneuver. Alli and Singh [9] designed passive controllers on a distributed parameter representation of the crane cable for point-

to-point maneuvers where the integral of the time absolute error is minimized. There have been numerous publications related to the use of input shapers [1], [10] for sway control of cranes [11], [12], [13], [14]. Shah and Hong [15] applied input shaping for the underwater transport of nuclear power plant's fuel.

This paper considers a gantry crane system driven by stepper motors which permits commanding the position of the trolley. Imposing velocity limits on the trolley motion, this paper considers the design of velocity constrained time-optimal point-to-point control of a crane moving in two dimensions. Since the pendular motion is almost undamped, an undamped system model will be first considered and observations of the structure of switching function is used to solve a nonlinear function to determine the optimal solution for any arbitrary maneuver. The solution is then extended to underdamped systems.

Section II presents the development of velocity constrained time-optimal control for an undamped gantry crane system followed by the same development for underdamped systems in Section III. Sections IV presents a simple approach to determine the transition in the structure of the control profile, followed by the development of a problem to desensitize the controller to model parameter uncertainties in Section V. The paper concludes with a brief summary of the results of the paper.

II. UNDAMPED SYSTEM

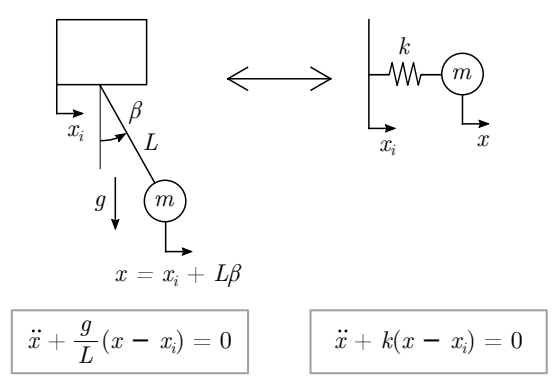


Fig. 1: Equivalent Spring Mass system

The gantry crane setup includes a trolley driven by a stepper motor which permits commanding a position. A schematic of the crane and an equivalent spring-mass system is shown in Fig. 1. The spring-mass model can be written

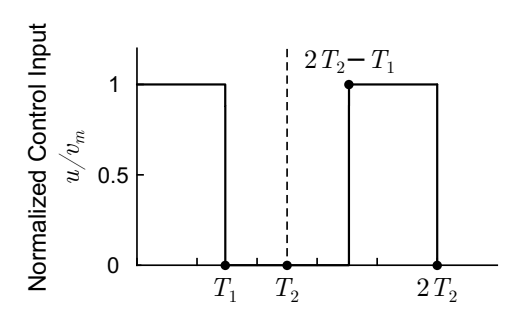
$$m\ddot{x} + kx - kx_i = 0 \tag{1}$$

$$\dot{x}_i = v \tag{2}$$

where v is the velocity of the trolley is considered as the input and is constrained $0 \le v \le v_m$. Mass normalization leads to the equation:

$$\ddot{x} + \omega_n^2 x = \omega_n^2 x_i \tag{3}$$

where we assume $\omega_n=2\pi$ to generate numerical results. For a rest-to-rest maneuver, we assume that the initial displacement $x(0)=\dot{x}(0)=x_i(0)=0$ and the terminal position is $x(t_f)=x_i(t_f)=x_f$ and $\dot{x}(t_f)=0$. Since the



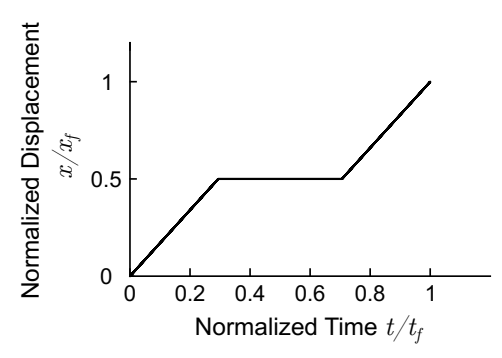


Fig. 2: Velocity and Displacement Profiles

input velocity is constrained, the time-optimal bang-off-bang control profile can be parameterized as the output of a time-delay filter $(G_c(s))$

$$v(s) = \frac{v_m}{s} \underbrace{\left[1 - e^{-sT1} + e^{-s(2T_2 - T_1)} - e^{-s2T_2}\right]}_{=G_c(s)} \tag{4}$$

subject to a unit step input. Since the system is undamped, we assume symmetry about the mid-maneuver time reducing the number of variables needed to parameterize the bang-off-bang control profile as shown in Fig. 2. As shown by Singh and Vadali [16], the time-delay filter is required to place zeros at the location of the poles of the plant. We can see that

$$G_c(s=0) = 1 - 1 + 1 - 1 = 0$$
 (5)

which cancels the pole at the origin. To cancel the undamped

poles at $s = j \omega_n$ we require:

$$1 - \cos(\omega_n T_1) + \cos(\omega_n (2T_2 - T_1)) \dots$$
 (6)

$$\dots - \cos(\omega_n 2T_2) = 0$$

$$\sin(\omega_n T_1) - \sin(\omega_n (2T_2 - T_1)) + \sin(\omega_n 2T_2) = 0 \quad (7)$$

which reduces to the constraint:

$$\sin\left(\omega_n\left(T_2 - T_1\right)\right) - \sin\left(\omega_n T_2\right) = 0. \tag{8}$$

Eq. (8) results in the closed form solution:

$$\pi - \omega_n(T_2 - T_1) = \omega_n T_2. \tag{9}$$

To satisfy the terminal rigid body displacement, we require:

$$x_f(2T_2) = \int_0^{t_f} v dt = 2T_1 v_m \tag{10}$$

$$\to T_1 = \frac{x_f}{2v_m}.\tag{11}$$

Using Eq. (9) and (11) leads to:

$$2T_2 = \frac{\pi}{\omega_n} + \frac{x_f}{2v_m}. (12)$$

Examining Eq. (9), one can conceive of a situation where the switch time T_1 coincides with the mid-maneuver time T_2 resulting in the solution:

$$T_2 = T_1 = \frac{\pi}{\omega_n} \tag{13}$$

Equating Eq. (11) and (13), we arrive at the specific displacement

$$x_f = \frac{2v_m \pi}{\omega_n} \tag{14}$$

for which the optimal control profile is a rectangular pulse of width $2T_2$. Fig. 3 illustrates the transition of the optimal control profile from a four-switch bang-off-bang to a bang profile, eventually leading to a six switch bang-off-bang control profile. To prove optimality, the time optimal control problem is formulated. The state space model of the system is:

$$\dot{x} = \dot{x}_1 = x_2 \tag{15a}$$

$$\ddot{x} = \dot{x}_2 = -\omega_n^2 x_1 + \omega_n^2 x_3 \tag{15b}$$

$$v = \dot{x}_3 = u \tag{15c}$$

$$0 \le u \le v_m. \tag{15d}$$

which permits the Hamilitonian to be written as

$$\mathcal{H} = 1 + \lambda_1 x_2 + \lambda_2 \left(-\omega_n^2 x_1 + \omega_n^2 x_3 \right) + \lambda_3 u \tag{16}$$

which leads to the equations for the costates and optimal control as:

$$\dot{\lambda}_1 = -\frac{\partial \mathcal{H}}{\partial x_1} = \omega_n^2 \lambda_2 \tag{17a}$$

$$\dot{\lambda}_2 = -\frac{\partial \mathcal{H}}{\partial x_2} = -\lambda_1 \tag{17b}$$

$$\dot{\lambda}_3 = -\frac{\partial \mathcal{H}}{\partial x_3} = -\omega_n^2 \lambda_2 \tag{17c}$$

$$u = \frac{\partial \mathcal{H}}{\partial u} = \lambda_3 = v_m H\left(-\lambda_3\right). \tag{17d}$$

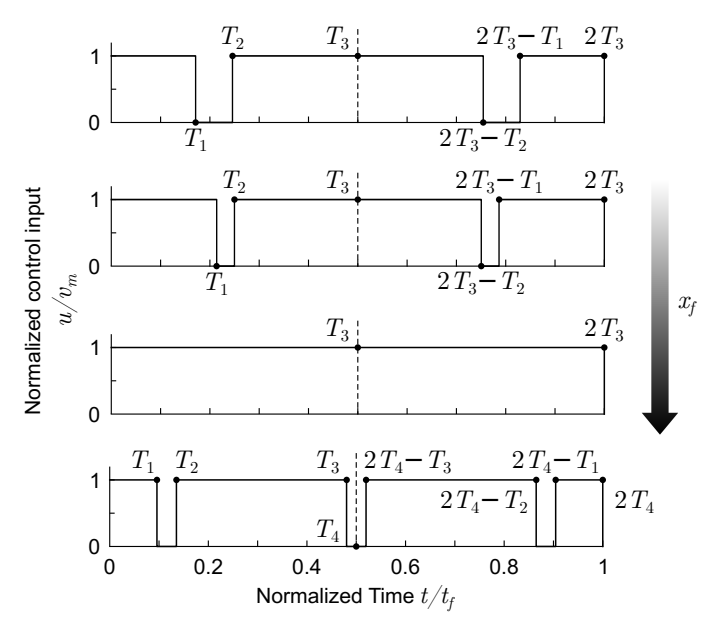


Fig. 3: Transition of Optimal Control profile

Since the velocity input is constrained to be positive, the optimal control profile is parameterized with the Heaviside function whose argument is the switching function:

$$\lambda_3(t) = -A\cos(\omega_n t) - B\sin(\omega_n t) + D \tag{18}$$

where A, B and D are parameters which need to be solved for. Due to the symmetry of the control profile, a collapse in T_1 and T_2 would lead to the following constraints $\lambda_3(T_1) = \dot{\lambda}_3(T_1) = \lambda_3(t_f - T_1) = \dot{\lambda}_3(t_f - T_1) = \lambda_3(0) = 0$. This in conjunction with the requirement that the Hamiltonian $\mathcal{H}(0) = 0$ results in the following expressions:

$$-A\cos(\omega_n T_1) - B\sin(\omega_n T_1) + D = 0 \tag{19a}$$

$$A\sin(\omega_n T_1) - B\cos(\omega_n T_1) = 0 \tag{19b}$$

$$-A\cos(\omega_n T_1) + B\sin(\omega_n T_1) + D = 0 \tag{19c}$$

$$-A\sin(\omega_n T_1) - B\cos(\omega_n T_1) = 0 \tag{19d}$$

$$-A + D = 0.$$
 (19e)

Eq. (19a) and Eq. (19c) can be satisfied simultaneously if B=0. Eq. (19b) and Eq. (19d) with B=0 results in $\omega_n T_1 = n\pi$, where n is an integer. This leads to $T_1 = \frac{n\pi}{\omega}$, which matches the early described observation because when the switches collapse $t_f=2T_2=2T_1=\frac{2n\pi}{\omega_n}$. Since the optimal two switch control profile collapses to a rectangular pulse which implies a ramp displacement profile, one can conjecture for larger displacements, a four switch control profile is necessary since the switching function completes one complete period for the critical displacement $x_f =$ $\frac{2v_m\pi}{r}$. Any increase in the commanded displacement requires a four switch bang-off-bang profile where the switch times coalesce for a final displacement of $x_f = \frac{4v_m\pi}{\omega_n}$ resulting in a rectangular optimal velocity profile. Fig. 4 illustrates the structure of the time-optimal control profile and the transition of the switch times and maneuver time as a function of the terminal displacement of the crane's trolley. The two vertical

dashed line correspond to the displacements which require no switches in the optimal control profiles. The filled regions of the graphs corresponds to the interval of times when the commanded velocity is the maximum and the white zones are ones where the commanded velocity is zero. Results presented assumed a maximum velocity limit of 240 mm/s.

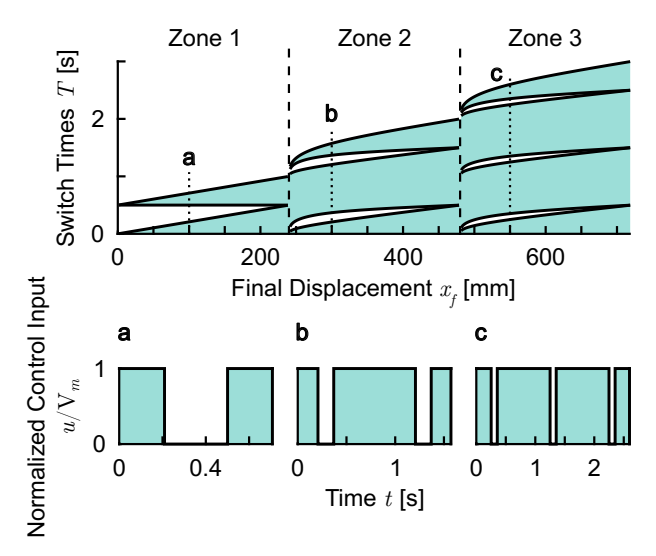


Fig. 4: Switch and Maneuver Time Variation

III. UNDERDAMPED SYSTEM

Section II dealt with undamped system which permitted a reduced order parameterization of the optimal control profile by exploiting the symmetric nature of the control about the mid-maneuver time. This symmetry is attributed to the fact that the oscillator motion excited by the input does not damp out and the symmetric input can by virtue of linearity of the system generate an out of phase motion of the undamped modes which cancels the existing oscillations. For a system with damping, the symmetric nature of the control profile is lost since the amplitude of the oscillatory mode decays in time. Consequently, the optimal control profiles needs to explicitly parameterize every switch in addition to the maneuver time. For instance for small displacements, the optimal control is parameterized as:

$$v(s) = \frac{v_m}{s} \underbrace{\left[1 - e^{-sT_1} + e^{-sT_2} - e^{-sT_3}\right]}_{=G_s(s)}.$$
 (20)

The constraints to identify the optimal values of T_1 , T_2 , and T_3 are derived by requiring the zeros of the time-delay filter to cancel the pole at the origin and the underdamped poles of the system. This results in the constraints:

$$G_c(s=0) = 1 - 1 + 1 - 1 = 0$$
 (21)

which cancels the pole at the origin. To cancel the underdamped poles at $s=-\sigma\pm j\;\omega_d=-\zeta\omega_n\pm j\;\omega_n\sqrt{1-\zeta^2},$ where $\zeta = 0.01$ we require:

$$1 + \sum_{i=1}^{3} (-1)^{i} e^{\sigma T_{i}} \cos(\omega_{n} T_{i}) = 0$$
 (22)

$$\sum_{i=1}^{3} (-1)^{i} e^{\sigma T_{i}} \sin(\omega_{n} T_{i}) = 0.$$
 (23)

To satisfy the terminal rigid body displacement, we require:

$$x(T_3) = x_f = \int_0^{t_f} v dt \tag{24}$$

$$= v_m \left(T_3 - (T_3 - T_1) + (T_3 - T_2) \right) \tag{25}$$

$$\to x_f = v_m (T_3 + T_1 - T_2). \tag{26}$$

The nonlinear optimization problem that needs to be solved is:

$$\min \ J = T_3 \tag{27a}$$

subject to

$$v_m (T_3 + T_1 - T_2) = x_f$$
 (27b)

$$1 + \sum_{i=1}^{3} (-1)^{i} e^{\sigma T_{i}} \cos(\omega_{n} T_{i}) = 0$$
 (27c)

$$\sum_{i=1}^{3} (-1)^{i} e^{\sigma T_{i}} \sin(\omega_{n} T_{i}) = 0$$
 (27d)

$$0 \le T_1 \le T_2 \le T_3. \tag{27e}$$

As in the case of the undamped system, the number of switches necessary to parameterize the optimal control profile changes with the terminal displacement. Fig. 5 illustrates the variation of the switch times as a function of the final displacement and the control input over the maneuver time for specific examples. For terminal displacements of 0-700 mm, three zones have been identified, separated by the vertical dashed lines. Three representative optimal control profiles are presented corresponding to three displacements highlighted by the dotted lines and labelled a, b and c. It is interesting to note that in zone 3 which includes the dotted line c, the number of switches required for the optimal control profile starts with four switches, transitions to six switches, and returns to a four switch optimal control profile.

IV. SWITCHING PROFILE TRANSITION

It is clear from Fig. 4 and 5 that the structure of bang-off-bang control profile changes as a function of the terminal displacement. In Fig. 4, for small displacements $(x_f \le 240 \text{ mm})$, the optimal control profile is characterized by two switches and the switches after collapsing resulting in a pulse control profile, births a four switch control profile which then transition to a six switch control profile. The change in structure of the optimal control profile for underdamped systems is more involved as all switches do not collapse for the same value of the terminal displacement. To exactly determine the terminal displacement which corresponds to the birth or collapse of two or more switches,

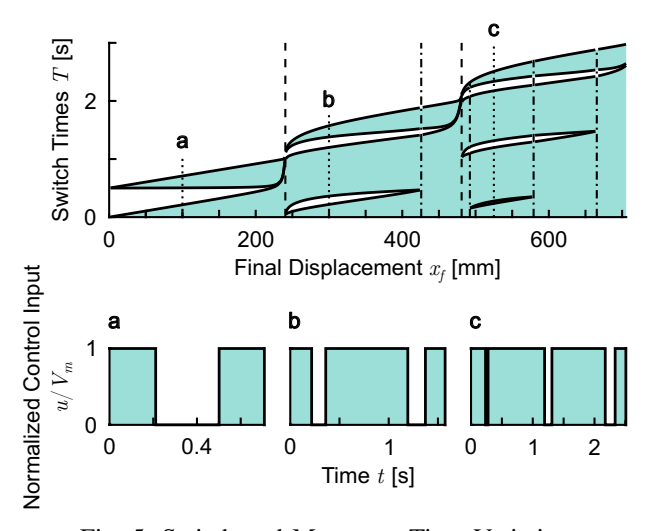


Fig. 5: Switch and Maneuver Time Variation

the constraint is that the switching function and its time derivative are simultaneously zero at some time instant. For the underdamped system the switching function $\lambda_3(t)$ can be represented as:

$$\lambda_3 (t_{cr}, x_f) = \dot{\lambda}_3 (t_{cr}, x_f) = 0.$$
 (28)

where t_{cr} is the switch time where two switches collapse. t_{cr} and x_f can be determined by solving the two nonlinear simultaneous equations in two unknowns while satisfying all the necessary conditions for optimality.

V. ROBUST CONTROL

The challenge of dealing with model parameter uncertainties is ubiquitous and there have been numerous approaches proposed for the design of robust open-loop controllers including enforcing robustness around the nominal model of the system or a minimax problem formulation where the maximum residual energy is minimized over an interval of uncertainty. In this work, we determine the sensitivity of the states of the system with respect to uncertainty in the spring stiffness and force the sensitivity states at the terminal time to be zero. The resulting state space model is:

$$\dot{x}_1 = x_2 \tag{29a}$$

$$\dot{x}_2 = -\omega_n^2 x_1 + \omega_n^2 x_3 \tag{29b}$$

$$\dot{x}_2 = -\omega_n^2 x_1 + \omega_n^2 x_3$$

$$\frac{d\dot{x}_1}{d\omega_n} = \frac{dx_2}{d\omega_n}$$
(29b)

$$\frac{d\dot{x}_2}{d\omega_n} = -2\omega_n x_1 - \omega_n^2 \frac{dx_1}{d\omega_n} + 2\omega_n x_3 \tag{29d} \label{eq:29d}$$

$$v = \dot{x}_3 = u \tag{29e}$$

$$0 \le u \le v_m. \tag{29f}$$

and is subject to the initial and final conditions:

$$x_1(0) = x_2(0) = x_3(0) = 0$$
 (30a)

$$\frac{dx_1}{d\omega_n}(0) = \frac{dx_2}{d\omega_n}(0) = 0 \tag{30b}$$

$$x_1(t_f) = x_3(t_f) = x_f,$$
 (30c)

$$x_2(t_f) = \frac{dx_1}{d\omega_n}(t_f) = \frac{dx_2}{d\omega_n}(t_f) = 0$$
 (30d)

Solving the robust velocity constrained time-optimal control problem for the undamped system for various terminal displacements, the variation in the optimal control profile as a function of the terminal displacement is illustrated in Fig. 6. Fig. 7 illustrates the variation of the residual

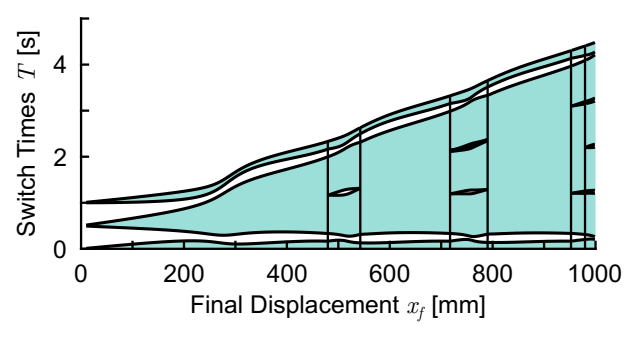


Fig. 6: Switch and Maneuver Time Variation for Robust Control

energy at the terminal time for the non-robust and robust time-optimal controllers over a range of uncertain natural frequencies for the undamped system. It is clear that the yellow line which represents the variation of residual energy of the robust control outperforms the non-robust design illustrated by the black line. These graphs are generated for a terminal displacement of 50 mm. Currently, a experimental

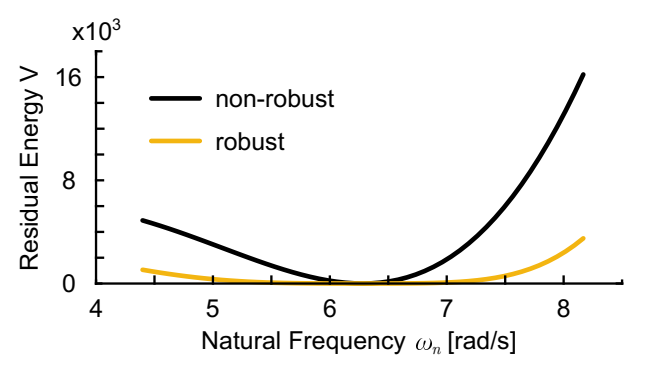


Fig. 7: Switch and Maneuver Time Variation for Robust Control for $x_f = 50 \text{ mm}$

setup is being constructed to test and validate the bang-offbang optimal control profiles with an ability to change the natural frequency of the system to gauge the robustness. Experimental results will be presented in a future paper.

VI. CONCLUSIONS

This paper presented a optimal control based development of a velocity limited time-optimal control of a gantry crane system which is characterized by one vibratory mode. The variation in the structure of the optimal control profile is presented for systems where the vibratory modes are undamped or underdamped. It is noted that as the final displacement increases, there is a increases in the number of switches in the optimal control profile with periodic terminal displacements requiring a pulse control profile with no switches. The optimal control framework can be easily extended to account for multiple vibratory modes such as when the crane is modelled as a double pendulum.

REFERENCES

- [1] N. C. Singer and W. P. Seering, "Preshaping command inputs to reduce system vibration," *Journal of Dynamic Systems, Measurement, and Control*, vol. 112, no. 1, pp. 76–82, 1990.
- [2] T. Singh, "Minimax design of robust controllers for flexible systems," Journal of guidance, control, and dynamics, vol. 25, no. 5, pp. 868– 875, 2002.
- [3] T. Singh, Ed., Jerk Limited Input Shapers. IEEE, 2004.
- [4] W. E. Singhose, A. K. Banerjee, and W. P. Seering, "Slewing flexible spacecraft with deflection-limiting input shaping," *Journal of Guid*ance, Control, and Dynamics, vol. 20, no. 2, pp. 291–298, 1997.
- [5] U. Staehlin and T. Singh, "Design of closed-loop input shaping controllers," in *Proceedings of the 2003 American Control Conference*, 2003., vol. 6. IEEE, 2003, pp. 5167–5172.
- [6] T. Vyhlídal, V. Kučera, and M. Hromčík, "Signal shaper with a distributed delay: Spectral analysis and design," *Automatica*, vol. 49, no. 11, pp. 3484–3489, 2013.
- [7] M. Noakes, B. Petterson, and J. Werner, "An application of oscillation damped motion for suspended payloads to the advanced integrated maintenance system," 1990.
- [8] M. Fliess, J. Levine, and P. Rouchon, "A simplified approach of crane control via a generalized state-space model," in [1991] Proceedings of the 30th IEEE Conference on Decision and Control. IEEE, 1991, pp. 736–741.
- [9] H. Alli and T. Singh, "Passive control of overhead cranes," *Journal of Vibration and Control*, vol. 5, no. 3, pp. 443–459, 1999.
- [10] T. Singh, Optimal reference shaping for dynamical systems: theory and applications. CRC Press, 2009.
- [11] S. Garrido, M. Abderrahim, A. Gimenez, R. Diez, and C. Balaguer, "Anti-swinging input shaping control of an automatic construction crane," *IEEE Transactions on Automation Science and Engineering*, vol. 5, no. 3, pp. 549–557, 2008.
- [12] N. Singer, W. Singhose, and E. Kriikku, "An input shaping controller enabling cranes to move without sway," Westinghouse Savannah River Co., Aiken, SC (United States), Tech. Rep., 1997.
- [13] W. Singhose, D. Kim, and M. Kenison, "Input shaping control of double-pendulum bridge crane oscillations," *Journal of Dynamic Systems, Measurement, and Control*, vol. 130, no. 3, 2008.
- [14] W. Singhose, L. Porter, M. Kenison, and E. Kriikku, "Effects of hoisting on the input shaping control of gantry cranes," *Control engineering practice*, vol. 8, no. 10, pp. 1159–1165, 2000.
- [15] U. H. Shah and K.-S. Hong, "Input shaping control of a nuclear power plant's fuel transport system," *Nonlinear Dynamics*, vol. 77, no. 4, pp. 1737–1748, 2014.
- [16] T. Singh and S. Vadali, "Robust time-optimal control-frequency domain approach," *Journal of Guidance, Control, and Dynamics*, vol. 17, no. 2, pp. 346–353, 1994.